RESEARCH PAPER

Preparation and Characterization of Electrospun (Polyacrylonitrile - Multi Wall Carbon Nanotubes) Nanofibers

*Mokhalad Ali Zbalh [1,2] *, A. Q. Abdullah [2], Alaa S. Alkabbi [2]*

[1] *Department of Genetic Engineering, Collage of Biotechnology, Al-Qasim Green University, Babylon, Iraq*

[2] *Department of Physics, College of Science, University of Basrah, Basrah, Iraq*

ARTICLE INFO

ABSTRACT

Composite nanofibers of polyacrylonitrile/ multi wall carbon nanotubes (PAN-MWCNTs) were prepared via electrospinning techniques using a moving collector. Samples contained 1 wt%, 3 wt%, 5 wt%, and 7 wt% of MWCNTs. Scanning electron microscopy, X-ray diffraction, Dielectric Properties and UV-visible tests were used to characterize the nanofiber sheets. The results showed that with the addition of multi-walled carbon nanotubes, the fiber diameter decrease, the bandgap decreased from 4 eV to 2.7 eV when the wight percent of MWCNTs increased.the dielectric constant values of PAN nanocomposite fibers increase based on the amount of inclusions presented in the PAN fibers.

How to cite this article

INTRODUCTION

Electrospinning utilizes a high electric field on the surface of a polymeric solution to overcome the surface tension and produce a very slim charged jet. A Polymeric solution is held by its surface tension at end the of the capillary stresses. As the intensity of the electrostatic field is increased beyond a certain limit, the hemispherical surface of the solution at the tip of the capillary elongates to form a structure called a Taylor cone[1]. The jet first extends in a straight path for some distance, called jet length[2], and then instability occurs and the jet bends and follows a looping path. The electrostatic field elongates the jet thousands of times and the jet becomes very slim. Finally, the solvent evaporates, and fine submicron fibers are collected on a collector placed at some distance from the capillary as shown in Fig. 1.

Polymer nanofiber papers have been fabricated using an electrospinning process that produces nanofibers from an electrically charged jet of polymer solution or polymer melts. The nanofiber diameters range from 40 nm to 2 mm, depending on the polymer types, bias voltage, viscosity of the solution, and so on[1]. One advantage of nanofibers is the high specific surface area developed by creating pores on the nanofiber surface[2]. Mechanical strength of an individual nanofiber is also expected to be enhanced with decreasing diameters[3]. This material has been widely applied to filters[4], scaffolds[5], protective clothing[6], and sensors[7].

Polyacrylonitrile (PAN) has been widely used to fabricate nanofibers owing to their easy carbonization process. PAN nanofiber papers can be used directly for electrode materials after

* *Corresponding Author Email: mokhaladali5@gmail.com*

stabilization and carbonization, which cannot be realized in other types of polymers. Another advantage of the carbonized PAN nanofiber is that; the nanofiber surface can be modified and functionalized by activation process under different ambient conditions[2].

Electrospinning is one of the effective methods to produce polymer nanofibers[1], [8]–[10], which have been successfully used as filters for air filtration,[11] as templates for making tubular nanostructures such as metal nanotubes[12], metal oxide nanotubes[13][14] or polymer nanotubes, [12][15] and as substrates for forming hierarchical carbon nanostructures. [16] Electrospun nanofibers are also finding uses in protective clothing,[17] nanocomposites,[18] optical sensors,[19] biomedical applications including biomedicine,[20], [21] scaffolding for tissue growth,[2], [22] drug delivery systems,[23] and for solar sails in space.[23] For macroscopic applications such as clothing, solar sails in space, or media for filtration, stronger polymer nanofibers are desired. However, the polymer nanofibers produced by electrospinning processes are not as strong as desired due to their very small diameters and the unoptimized molecular orientation in the fibers. Stretching and making composites can improve the mechanical properties of polymer fibers, but making nanocomposites is a more promising way to reinforce the nanofibers. Methods to stretch nanofibers are not available.

Carbon nanotubes (CNT), first reported by Iijima in 1990,[24] possess excellent mechanical properties and good electrical and thermal conductivity, making CNTs an ideal material for reinforcing polymer materials. Several reports were published on polymer materials reinforced by using CNTs.[25]–[29] The modulus and tensile strength were improved from several percent up to more than 100 percent, depending on the polymer matrix, types and synthesis methods of CNT, and concentration of the CNT in the matrix. Recently, Dror et al.[30] reported electrospun polyethylene oxide nanofibers containing low concentrations of multiwall CNTs (MWCNT),which were observed using transmission electron microscopy (TEM). In the work reported here, polyacrylonitrile nanofibers (PAN) containing MWCNT were produced in concentrations of (1, 3,5,7) wt%. Thick sheets of nanofibers were made. This work showed that at high concentration, MWCNTs were nearly parallel, along the axis of the nanofibers, embedded within the nanofibers. The optical properties tests showed that the energy gap decreased well, and the measurements of the dielectric constant were observed to increase with the increase of MWCNTs.

MATERIALS AND METHODS
Materials
Polyacrylonitrile (PAN) having molecular Weight 150,000g/mole was purchased from sigma Aldrich. MWCNTs were purchased from Fisher Scientific having diameter of 140 (+/- 30) nm and a length of 7 (+/- 2) microns.

Electrospinning process
Different wt. % (1%,3%, 5% and 7%) of MWCNTs were dissolved in Dimethylformamide (DMF) and Sonicated for 30 minutes Then PAN was added, and the solution was constantly stirred at 40 0C for 12h.The (PAN/DMF) + MWCNTs polymer solution
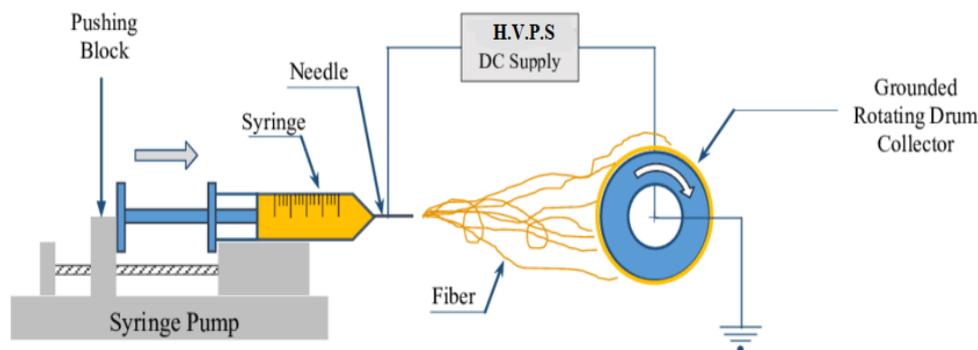

Fig. 1. Scheme Electrospinning device

was poured to fill a clean syringe of 3ml volume. The syringe(24g) needle was connected to the high voltage power supply at 10 kV of positive potential. A drum collector was centered horizontal at a 10 cm distance away from the needel of srying and covered with aluminum foil. The electrospun fibers were collected for about 6 h.

Characterization

Scanning Electron Microscopy (FESEM, TESCN MIRA3 FRENCH) was used for measuring the morphology of the composite nanofibers. The X-ray diffraction (XRD) in a Rigaku X-ray diffractometer operated with CuKα radiation (α = 1.540Å) is used for examined the structural characterization. UV visible spectroscopy (Shimazdu UV-1800) is used to make a characterization of the absorption, transmission and band gap of the composite nanofibers. Image processing software (Image J) was used to measure the diameters of the fiber.
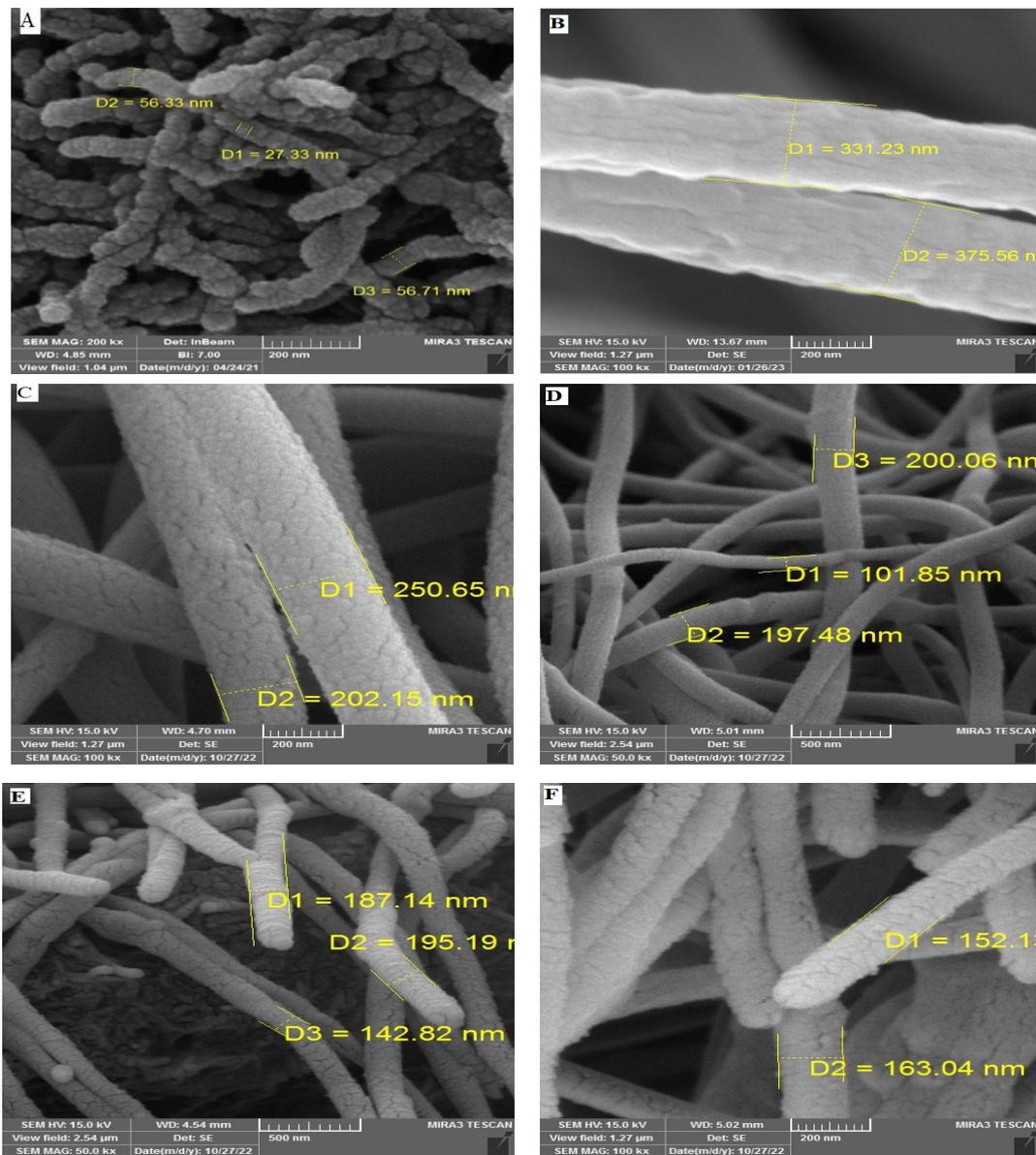

Fig. 2. Scanning electron microscopic images of the PAN-MWCNT composite nanofibers. (A) MWCNTs (B) PAN nanofibers; (C) contains 1% MWCNT by weight; (D) 3%; (E) 5%; (F) 7%

Table 1. The Fiber diameters range with MWCNT weight percent from SEM measurements.

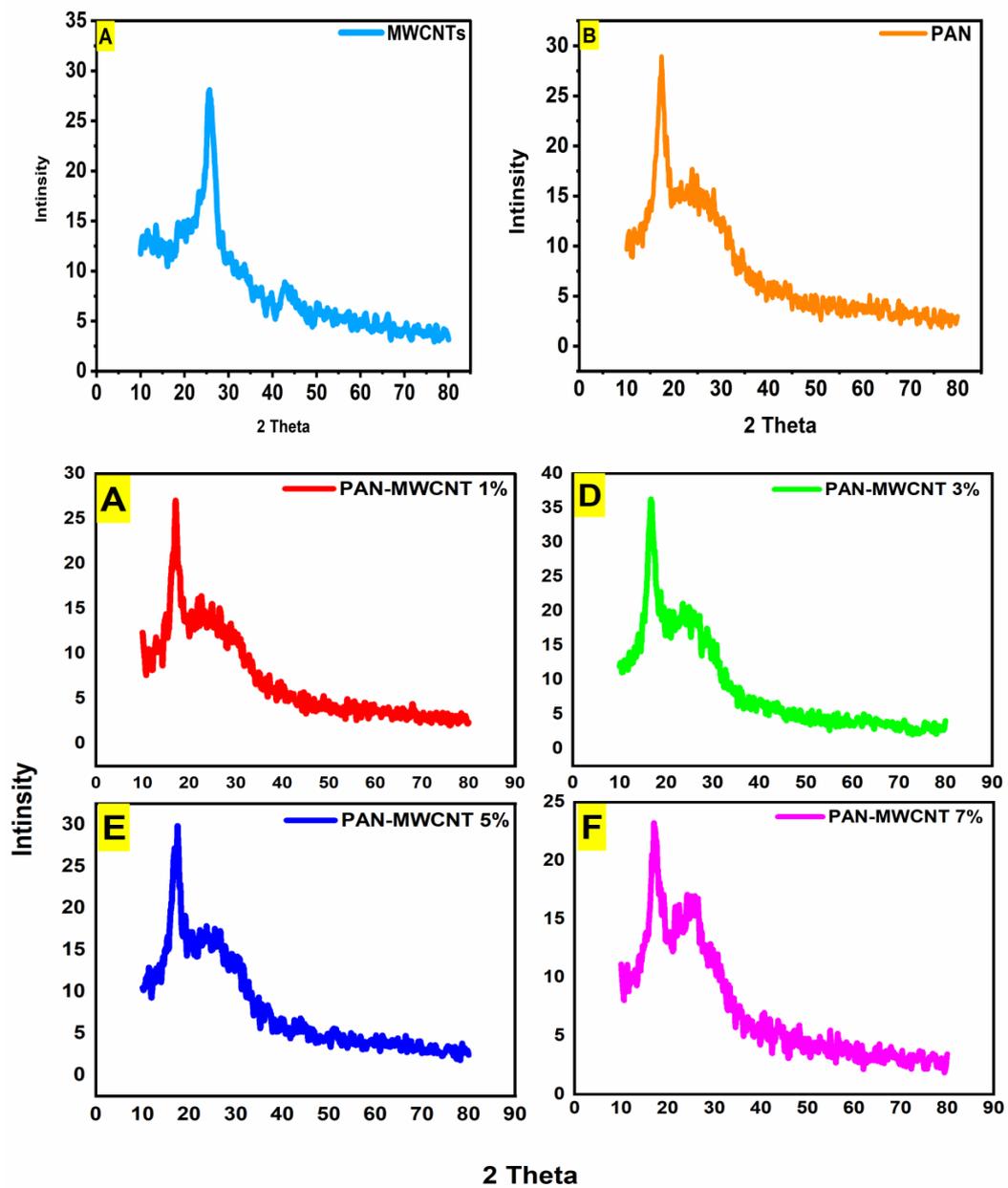| Material	Fiber diameters range (nm)
MWCNTs	27.33-56.71 nm
PAN	331 – 375 nm
PAN:MWCNTs 1%	202 – 250 nm
PAN:MWCNTs 3%	101 – 200 nm
PAN:MWCNTs 5%	142 -195 nm
PAN:MWCNTs 7%	152 - 163 nm

Fig. 3. XRD of MWCNT (A), PAN (B) and PAN-MWCNT composite nanofiber sheets containing MWCNT of 1% (C), 3% (D), 5% (E) and 7% (F) by weight, respectively.

The dielectric its measuring by PRPGRAMMABLE AUTOMATIC RCL METER.

RESULTS AND DISCUSSION

SEM measurements

The diameter of the fibers and the surface morphology of the composite nanofiber film can be observed by using the scanning electron microscopy (SEM). Fig. 2 shows the SEM images of PAN and PAN/MWCNT composite nanofibers with different concentration of MWCNT. Fig. 2a show the diameters of MWCNTs with range (27.33-56.71) nm[31]. Fig. 2b shows a very smooth, uniform and clear surface of PAN nanofiber with a spun fiber diameters range between from 331 to 375 nm. In Fig. 2(c–f), there are a different concentration of MWCNT in PAN composite nanofiber, a small beads and groups of CNT on the fiber was observed in Fig. 2(c–d). Moreover, Fig. 2d and e shows that there are bulges and many groves in the fiber web and it has been found that a group of CNTs pulled out of the fiber surface. The spun fibers diameters range are shown in Table1. As observed, the fiber diameter decrease as the
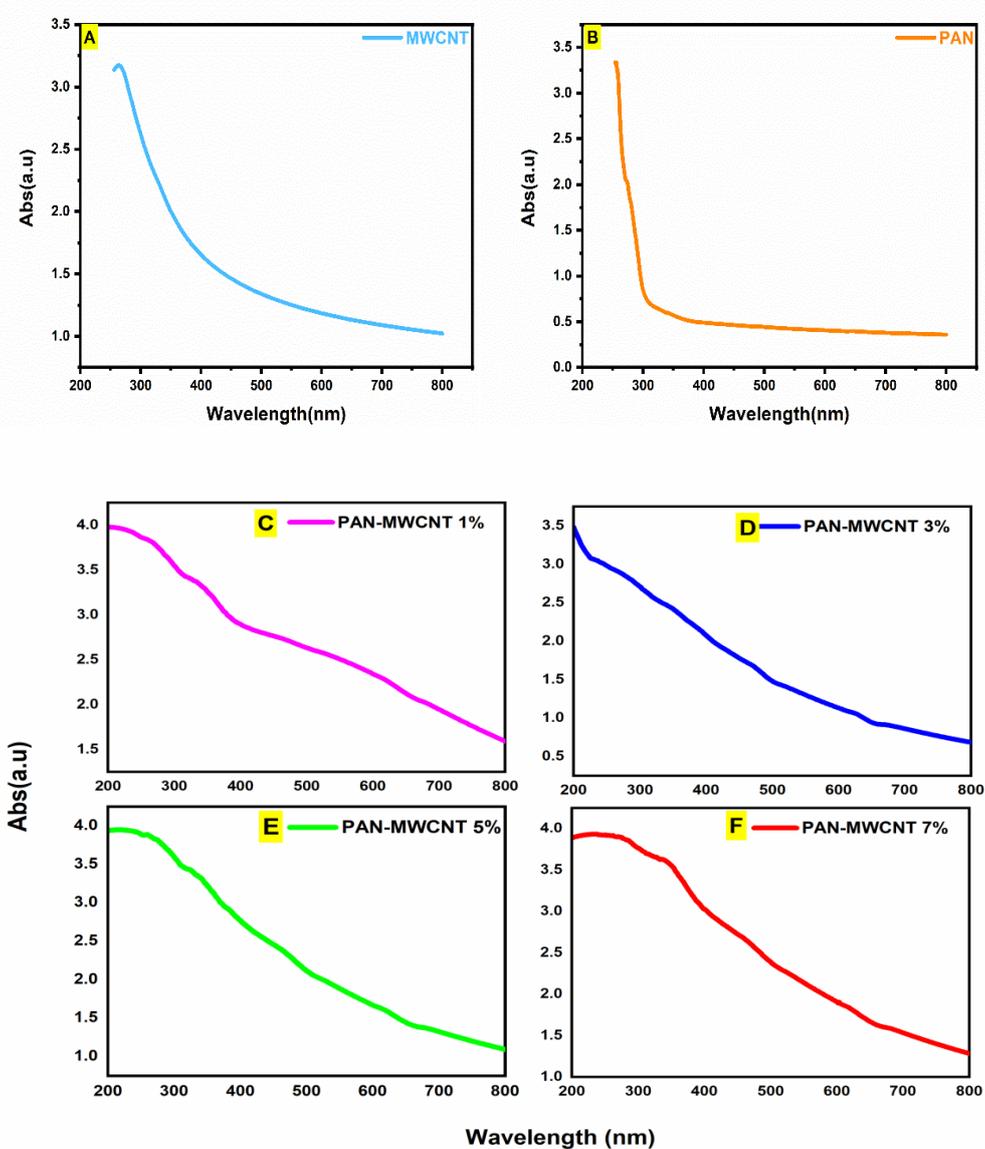

Fig. 4. Absorption spectra of MWCNT (A), PAN (B) and PAN-MWCNT composite nanofiber sheets (C-F)

MWCNT concentration is increased which can be attributed to increase in the PAN/MWCNT solution conductivity when the carbon precents increased.

X-ray diffraction analysis

XRD analysis was used to examine the phase structures of the composite nanofiber and the main PAN nanofibers which presented in Fig. 3. Fig. 3b is for the neat PAN nanofiber sheet. A strong peak was observed at 2θ =17.3°. This peak of diffraction can be assigned as (200) crystal planes of PAN. MWCNTs (Fig. 3a) exhibited a sharp, high intensity peak at 2θ =25.6∘ and lower intensity peak at 43.2∘, all of which were attributed to the diffraction signature of the distance between the walls of CNTs and the inter wall spacing [32]. For PAN-MWCNTs (Fig. 3c) the X-ray pattern showed both the characteristic peaks of PAN and the peaks of MWCNTs. The peaks of MWCNTs have been increased when the MWCNTs percent increased.

Optical characterization

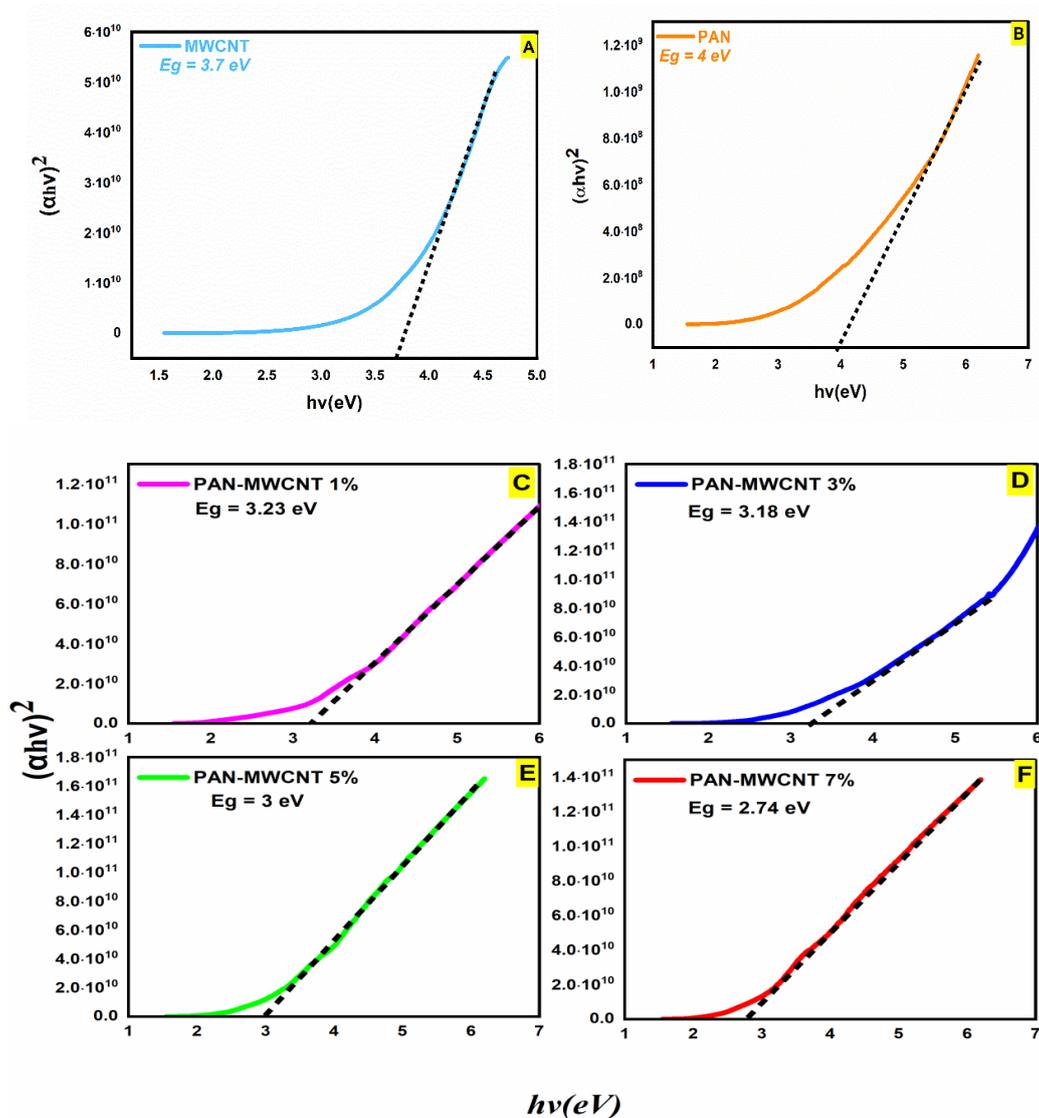UV–Visible is a fundamental tool to examine the optical properties and to distinguish electronic

Fig. 5. Band gap of MWCNT (A), PAN (B) and PAN-MWCNT composite nanofiber sheets containing MWCNT of 1% (C), 3% (D), 5% (E) and 7% (F) by weight, respectively

transitions. The UV–Visible spectra of the PAN/MWCNT nanocomposites with different weight ratios are shown in Fig. 4.

Fig. 4a shows the UV–Visible spectra of MWCNT. It indicates a strong absorption band at 260 nm attributed to n-π* transition [33].

The absorption spectra of neat PAN show high absorption at 260 nm and decreased with increasing of wavelength to 350 nm and becomes stable at higher wavelengths. This band is attributed to the electronic transitions n-π*[34]. Also, the low absorption of PAN above 350 nm means that the free-standing film of PAN is transparent to the entire visible wavelength above 300 nm. It well be shown also that the absorbance of these nanocomposites increases by MWCNT concentration increasing [35] .

The optical band gap of neat PAN and its nanocomposites were determined by translating the UV–Visible Spectra into Tauc's plot [36] and were estimated from the intercept of the extrapolated linear part of the plot of $(\alpha h)^{1/n}$ versus the photon energy with abscissa.

$$(\alpha h\nu) = B(h\nu - E_g)^n \qquad (1)$$

α: is the absorption coefficient, B is a parameter that depends on the interband transition, hν is the incident photon energy, E_g is the optical band gap and n is an index characterizing the nature of the electronic transition which causes the optical absorption. The n index can be equal to 1/2, 3/2, 2, 3 for direct allowed, direct forbidden, indirect allowed and finally indirect forbidden transitions respectively.

The values of the optical band gap are illustrated in Fig. 5 from which (and its inset) we can notice a decrease of the band gap energy from 4 eV to 2.7 eV. This decrease in band gap infers that the addition of MWCNT modifies the electronic structure of PAN molecules and may be the result of two mechanisms. The first is the creation of new levels in the band gap which facilitates the electrons moving from valence band to conduction band [24]. The second mechanism is the formation of defects in the polymer matrix. These defects can produce localized states at the
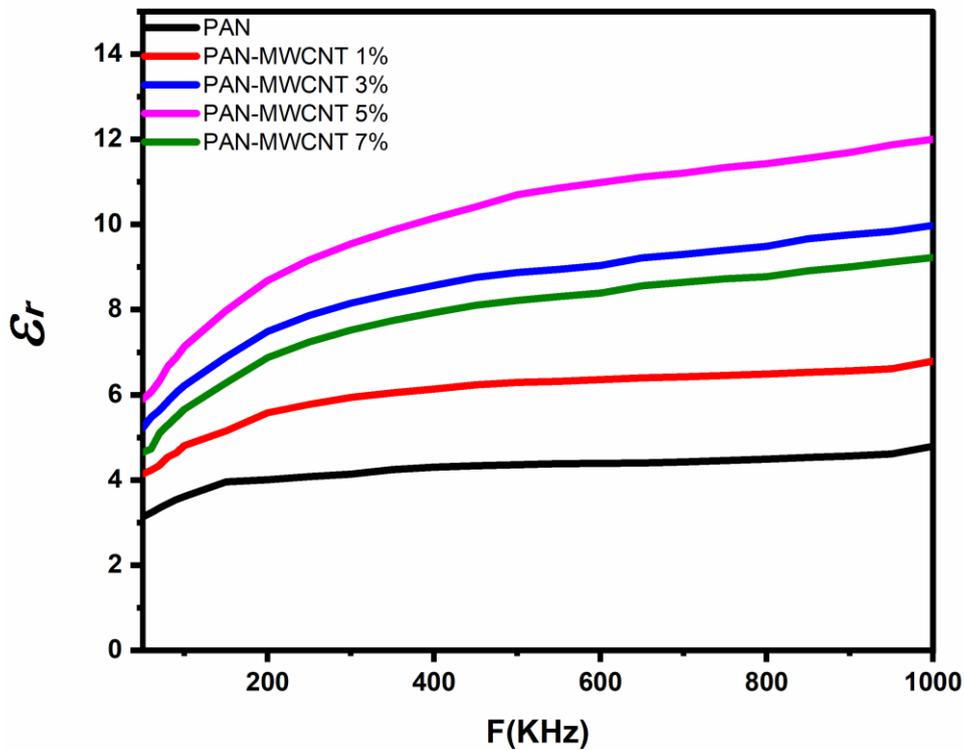

Fig. 6. Dielectric constant of PAN with different weight % of MWCNTs VS frequency

level of the optical band gap and these localized states are responsible for this decrease.

Dielectric Constant

The dielectric measurement results of neat PAN and PAN-MWCNT nanocomposite thin films are shown in Fig. 6. As can be seen, dielectric constant values of PAN nanocomposite fibers increase based on the amount of inclusions presented in the PAN fibers. The dielectric properties of a polymer depend on several factors, including temperature, frequency, structure, composite of polymers polar and nonpolar, inclusions, moisture, and defects. MWCNT is conducting materials, while PAN are electrical insulators. This means that MWCNTs have higher free charge concentrations at room temperature than PAN fibers. Therefore, the addition of MWCNT increases the number of dipole moments in the nanocomposite system. This leads to the increasing polarizability of the nanocomposite fibers with increasing wt % of MWCNTs. The relation between the dielectric constant r and the molecular polarizability t is given by

$$\varepsilon_r = 1 + \left(\frac{N\alpha t}{\varepsilon_o}\right) \tag{2}$$

Where N is the concentration of molecules and is the permittivity of free space. According to this relation, the dielectric constant should increase by increasing the polarizability of the material, which comes from the nanoscale inclusions in the fibers.

In this experiment, the dielectric readings were taken based on the assumption of uniform thickness of the samples, uniform dispersion of MWCNTs and moisture free samples. A part from these factors, porosity and air pockets present in the fiber texture also play an important role in altering the dielectric properties of nanocomposite fibers. The values of dielectric constant of materials in fibrous form are lower than their bulk forms because of air pockets present in fiber texture and nanoscale inclusions embedded into the polymers.

CONCLUSION

In conclusion, the study demonstrates that the incorporation of multi-walled carbon nanotubes (MWCNTs) into polyacrylonitrile (PAN) significantly influences the morphological, structural, optical, and dielectric properties of the resulting composite nanofibers. The findings indicate that increasing MWCNT concentration not only enhances the conductivity and polarizability of the nanocomposite but also modifies its electronic structure, leading to a notable decrease in the optical band gap and an increase in the dielectric constant, thereby highlighting the potential applications of these materials in advanced technological fields.

CONFLICT OF INTEREST

The authors declare that there is no conflict of interests regarding the publication of this manuscript.

REFERENCES

1. Reneker DH, Chun I. Nanometre diameter fibres of polymer, produced by electrospinning. Nanotechnology. 1996;7(3):216-223.
2. Li WJ, Laurencin CT, Caterson EJ, Tuan RS, Ko FK. Electrospun nanofibrous structure: A novel scaffold for tissue engineering. J Biomed Mater Res. 2002;60(4):613-621.
3. Keun Kwon I, Kidoaki S, Matsuda T. Electrospun nano- to microfiber fabrics made of biodegradable copolyesters: structural characteristics, mechanical properties and cell adhesion potential. Biomaterials. 2005;26(18):3929-3939.
4. Tsai PP, Schreuder-Gibson H, Gibson P. Different electrostatic methods for making electret filters. J Electrostatics. 2002;54(3-4):333-341.
5. Fertala A, Han WB, Ko FK. Mapping critical sites in collagen II for rational design of gene-engineered proteins for cell-supporting materials. J Biomed Mater Res. 2001;57(1):48-58.
6. Gibson PW, Schreuder-Gibson HL, Rivin D. Electrospun fiber mats: Transport properties. AIChE Journal. 1999;45(1):190-195.
7. Ding B, Kim J, Miyazaki Y, Shiratori S. Electrospun nanofibrous membranes coated quartz crystal microbalance as gas sensor for NH3 detection. Sensors Actuators B: Chem. 2004;101(3):373-380.
8. Baumgarten PK. Electrostatic spinning of acrylic microfibers. Journal of Colloid and Interface Science. 1971;36(1):71-79.
9. Jaeger R, Schönherr H, Vancso GJ. Chain Packing in Electro-Spun Poly(ethylene oxide) Visualized by Atomic Force Microscopy. Macromolecules. 1996;29(23):7634-7636.
10. Reneker DH, Yarin AL, Fong H, Koombhongse S. Bending instability of electrically charged liquid jets of polymer solutions in electrospinning. J Appl Phys. 2000;87(9):4531-4547.
11. Antibacterial Polymeric Nanofibers from Zwitterionic Terpolymers by Electrospinning for Air Filtration. American Chemical Society (ACS).
12. Bognitzki M, Hou H, Ishaque M, Frese T, Hellwig M, Schwarte C, et al. Polymer, Metal, and Hybrid Nano- and Mesotubes by Coating Degradable Polymer Template Fibers (TUFT Process). Adv Mater. 2000;12(9):637-640.
13. Caruso RA, Schattka JH, Greiner A. Titanium Dioxide Tubes from Sol–Gel Coating of Electrospun Polymer Fibers. Adv

Mater. 2001;13(20):1577.

14. Caruso RA, Schattka JH, Greiner A. ChemInform Abstract: Titanium Dioxide Tubes from Sol-Gel Coating of Electrospun Polymer Fibers. ChemInform. 2001;32(51).

15. Hou H, Jun Z, Reuning A, Schaper A, Wendorff JH, Greiner A. Poly(p-xylylene) Nanotubes by Coating and Removal of Ultrathin Polymer Template Fibers. Macromolecules. 2002;35(7):2429-2431.

16. Hou H, Reneker DH. Carbon Nanotubes on Carbon Nanofibers: A Novel Structure Based on Electrospun Polymer Nanofibers. Adv Mater. 2004;16(1):69-73.

17. Gibson P, Schreuder-Gibson H, Rivin D. Transport properties of porous membranes based on electrospun nanofibers. Colloids Surf Physicochem Eng Aspects. 2001;187-188:469-481.

18. Bergshoef MM, Vancso GJ. Transparent Nanocomposites with Ultrathin, Electrospun Nylon-4,6 Fiber Reinforcement. Adv Mater. 1999;11(16):1362-1365.

19. Wang X, Drew C, Lee S-H, Senecal KJ, Kumar J, Samuelson LA. Electrospun Nanofibrous Membranes for Highly Sensitive Optical Sensors. Nano Lett. 2002;2(11):1273-1275.

20. Hou H, Ge JJ, Zeng J, Li Q, Reneker DH, Greiner A, et al. Electrospun Polyacrylonitrile Nanofibers Containing a High Concentration of Well-Aligned Multiwall Carbon Nanotubes. Chem Mater. 2005;17(5):967-973.

21. Incorporation of Gentamicin-Encapsulated Poly(lactic-co-glycolic acid) Nanoparticles into Polyurethane/Poly(ethylene oxide) Nanofiber Scaffolds for Biomedical Applications. American Chemical Society (ACS).

22. Matthews JA, Wnek GE, Simpson DG, Bowlin GL. Electrospinning of Collagen Nanofibers. Biomacromolecules. 2002;3(2):232-238.

23. Kenawy E-R, Bowlin GL, Mansfield K, Layman J, Simpson DG, Sanders EH, et al. Release of tetracycline hydrochloride from electrospun poly(ethylene-co-vinylacetate), poly(lactic acid), and a blend. Journal of Controlled Release. 2002;81(1-2):57-64.

24. Iijima S. Helical microtubules of graphitic carbon. Nature. 1991;354(6348):56-58.

25. Gong X, Liu J, Baskaran S, Voise RD, Young JS. Surfactant-Assisted Processing of Carbon Nanotube/Polymer Composites. Chem Mater. 2000;12(4):1049-1052.

26. Zhang X, Liu T, Sreekumar TV, Kumar S, Moore VC, Hauge RH, et al. Poly(vinyl alcohol)/SWNT Composite Film. Nano Lett. 2003;3(9):1285-1288.

27. Vigolo B, Poulin P, Lucas M, Launois P, Bernier P. Improved structure and properties of single-wall carbon nanotube spun fibers. Appl Phys Lett. 2002;81(7):1210-1212.

28. Kumar S, Dang TD, Arnold FE, Bhattacharyya AR, Min BG, Zhang X, et al. Synthesis, Structure, and Properties of PBO/SWNT Composites. Macromolecules. 2002;35(24):9039-9043.

29. Thostenson ET, Chou T-W. Aligned multi-walled carbon nanotube-reinforced composites: processing and mechanical characterization. J Phys D: Appl Phys. 2002;35(16):L77-L80.

30. Dror Y, Salalha W, Khalfin RL, Cohen Y, Yarin AL, Zussman E. Carbon Nanotubes Embedded in Oriented Polymer Nanofibers by Electrospinning. Langmuir. 2003;19(17):7012-7020.

31. Carbon Nanotube-Adsorbed Polystyrene and Poly(methyl methacrylate) Microspheres. American Chemical Society (ACS).

32. Saito Y, Yoshikawa T, Bandow S, Tomita M, Hayashi T. Interlayer spacings in carbon nanotubes. Physical Review B. 1993;48(3):1907-1909.

33. Aziz SB, Rasheed MA, Hussein AM, Ahmed HM. Fabrication of polymer blend composites based on [PVA-PVP]$_{(1-x)}$(Ag$_2$S) x (0.01 ≤ x ≤ 0.03) with small optical band gaps: Structural and optical properties. Mater Sci Semicond Process. 2017;71:197-203.

34. Shoubak WM, Hassan A, Mahrous S, Hassen A. Controlling the physical properties of polyacrylonitrile by strontium hexaferrite nanoparticles. Polym Bull. 2023;81(1):697-718.

35. Khalid AH, Abdulsattar MA, Hussain ZT, Jabor AA. The effect of different multiwall carbon nanotubes concentration on morphology, optical, and electrical properties used as flexible anode. Journal of Physics: Conference Series. 2020;1660(1):012054.

36. Tauc J, Menth A, Wood DL. Optical and Magnetic Investigations of the Localized States in Semiconducting Glasses. Phys Rev Lett. 1970;25(11):749-752.